Global rates and patterns of channel migration in river deltas

Teresa Jarriel[a,b], John Swartz[a,b], and Paola Passalacqua[a,b,1]

[a]Department of Civil, Architectural and Environmental Engineering, The University of Texas at Austin, Austin, TX 78758; and [b]Center for Water and the Environment, The University of Texas at Austin, Austin, TX 78758

Edited by Andrea Rinaldo, Ecole Polytechnique Federale de Lausanne, Lausanne, Switzerland, and approved September 30, 2021 (received for review February 16, 2021)

River deltas are dynamic systems whose channels can widen, narrow, migrate, avulse, and bifurcate to form new channel networks through time. With hundreds of millions of people living on these globally ubiquitous systems, it is critically important to understand and predict how delta channel networks will evolve over time. Although much work has been done to understand drivers of channel migration on the individual channel scale, a global-scale analysis of the current state of delta morphological change has not been attempted. In this study, we present a methodology for the automatic extraction of channel migration vectors from remotely sensed imagery by combining deep learning and principles from particle image velocimetry (PIV). This methodology is implemented on 48 river delta systems to create a global dataset of decadal-scale delta channel migration. By comparing delta channel migration distributions with a variety of known external forcings, we find that global patterns of channel migration can largely be reconciled with the level of fluvial forcing acting on the delta, sediment flux magnitude, and frequency of flood events. An understanding of modern rates and patterns of channel migration in river deltas is critical for successfully predicting future changes to delta systems and for informing decision makers striving for deltaic resilience.

river deltas | channel migration | global change | coastal morphodynamics

River deltas are globally ubiquitous wherever a river discharges into a body of water that is not capable of fully dispersing the incoming sediment load. Delta channels can widen, narrow, laterally migrate, meander, and avulse through time to adjust the existing surface channel network (1–4). Channel migration can be disruptive to human inhabitants living near channel banks, impact aquaculture and agriculture operations dependent on the location of proximal channels, and have major implications for engineering operations such as infrastructure design, bridge construction, land management practices, and flood planning (5, 6). In addition to affecting the hundreds of millions of people and associated human infrastructure on these systems, changes to channel networks can also have significant effects on the propagation and distribution of water, solutes, and solids throughout the network and on the ecosystems within and surrounding the channels (7–12). While significant advancements have been made in understanding both general and local drivers of channel mobility in specific systems (13–17), a synoptic measurement of current rates of delta channel mobility globally has not been attempted due to the lack of efficient tools to do so over such large spatial scales. Understanding the modern rates of surficial channel change in deltas globally is a crucial component in better informing future delta sustainability (18). Here, we develop a method for the automated extraction of channel migration rates from remotely sensed imagery using a combined deep learning and particle imaging velocimetry (PIV) approach. We then implement our method and analyze channel kinematics of 48 of the world's river deltas in order to correlate patterns in migration to forcings on each system over decadal timescales.

Numerous studies have provided insights into the processes driving channel lateral mobility and to migration rates over various timescales using field studies, interpretation of fluvial deposits, or time-lapse satellite imagery (13, 16, 19). However, accurate comparison of multiple systems is challenging due to differences in individual study approaches and lack of a consistent measurement timescale that can both result in significant apparent migration rate deviations (20). Global classification of deltas by geomorphic process and extant form has been an area of intense interest for decades (21), and recent work has made advances in quantifying the relative balance of river, tidal, and wave forcings for the majority of the world's deltas (22). Additionally, the relative vulnerability of deltas globally has been assessed to identify which systems are most at risk to factors including land loss, riverine flooding, and storms (6, 23). These observations of historical and modern processes have helped inform predictions of how deltas may change in the future under different scenarios of sea-level rise, sediment flux, and flood recurrence intervals (24, 25). Although these studies provide information on the current status of river deltas and how they could potentially change, there are currently no global measurements capturing the actual rates of channel activity on deltas and assessing their change over the period of global satellite imagery.

Rates of morphologic change in channels can be potentially affected by a variety of forcings across a wide range of scales. From the construction of an individual dam to the influence of global-scale weather phenomena, channels can adjust in response to forcings. Although we cannot thoroughly account for all of the potential drivers of global geomorphic change due to a lack

Significance

River deltas are home to hundreds of millions of people and are currently undergoing natural and anthropogenically forced changes to their channel networks. It is important to document current decadal rates of delta channel migration to develop a better understanding of what global-scale phenomena exert influence on rates of change. We can then use that information to predict how future changes will continue to affect deltas and those who inhabit them. After extracting channel migration vectors from 48 deltas, we reconcile rates of migration with magnitudes of fluvial forcing, sediment flux, and flood frequency. By embedding the findings of this study in delta management strategies, a balance between human habitation and the natural dynamics of deltas can potentially be reached.

Author contributions: T.J. and P.P. designed research; T.J. and P.P. performed research; T.J., J.S., and P.P. analyzed data; and T.J., J.S., and P.P. wrote the paper.

The authors declare no competing interest.

This article is a PNAS Direct Submission.

[1]To whom correspondence may be addressed. Email: paola@austin.utexas.edu.

This article contains supporting information online at https://www.pnas.org/lookup/suppl/doi:10.1073/pnas.2103178118/-/DCSupplemental.

Published November 8, 2021.

of sufficient data, three factors are well known to directly influence migration rates: the balance of dominant processes (river, tidal, wave) (4, 17, 26–28), sediment flux magnitude (14, 29–31), and frequency of flood events (32–35). Specifically, studies have shown that when comparing fluvially dominated channels with tidally dominated channels, the tidally dominated zones display lower rates of movement (4, 17, 26–28). Thus, we may expect fluvially dominated systems to exhibit larger migration rates on a global scale as well. In addition to the influence of fluvial, tidal, and wave energies, the presence of sufficient magnitude of water and sediment also drives geomorphic change (14). Increases in the amount of sediment delivered to a channel can create bed changes that modify flow fields and promote channel migration (14, 36–39). Flood events that initiate the movement of large amounts of sediment can also cause morphological adjustments to channels. Therefore, we will examine how changes to flooding recurrence and sediment flux magnitudes are reflected in channel migration patterns globally. A fourth aspect that will potentially play a large role in channel migration is the average size of a delta's channels; larger channels may migrate farther in comparison with smaller channels as they have a greater capacity for geomorphic change. For reasons discussed in the following sections, here we will not globally analyze the impact of delta channel size on channel migration.

In this study, we create a classification system of decadal-scale channel kinematics that allows for the direct comparison of migration rates of deltas distributed globally. We then compare migration rates with the level of river forcing, magnitude of fluvial sediment flux, and flood frequency in each delta system. By quantifying delta channel migration patterns globally using this technique, we can provide necessary data to help inform assessments of delta sustainability and vulnerability and aid in improving predictions of future delta change under various environmental forcings.

Global Patterns of Channel Migration

By using a combination of deep learning and PIV image processing methods, we automate the extraction of channel migration rates from Landsat imagery at a high spatial resolution. We choose a previously compiled set of 48 major delta systems at risk spanning a diverse range of climate, biome, and socioeconomic contexts (23). For each delta, binary channel maps and channel centerlines are extracted from the oldest and the most recent clear images in the Landsat archive by using a combination of deep learning methods (40, 41) and morphological operators (42). A spatially dense set of migration vectors representing migration as meters per year is obtained from the two extracted channel centerline networks by applying the principles of PIV. Although in the past PIV has typically been used in turbulence studies to visualize the movement of fluids (43), here we apply it to real-world channel centerline networks in order to rapidly and accurately determine the entire spatial distribution of channel centerline displacements within a delta, regardless of size or complexity. We find that our PIV-enabled migration measurement technique is able to accurately capture vectors for mechanisms such as lateral migration, meandering, and translation, an improvement over previous methods for migration rate analysis (13, 16, 44–47).

Relative River, Tidal, and Wave Processes. In order to examine patterns between channel migration and the balance of dominant processes, median migration rates for each system are mapped onto a ternary diagram that allows for the visualization of the balance of river, tidal, and wave influences on river deltas (Fig. 1) (21, 22). We observe that all of the largest migration rates (greater than 3 m/y) fall into the river-dominated portion of the triangle. This suggests that a strong river forcing may be necessary for a river delta to have comparatively large migration

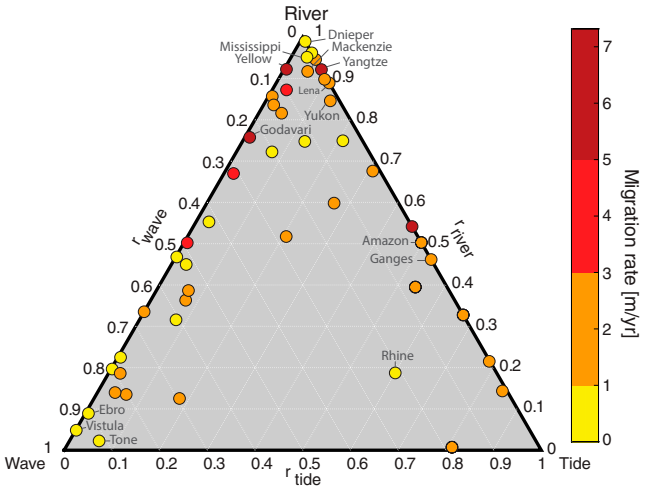

Fig. 1. Ternary plot of migration rate with relative wave, tidal, and river influence. Values for the relative river, wave, and tide forcings (r_{river}, r_{wave}, and r_{tide}, respectively) were obtained from Nienhuis et al. (22).

rates over decadal timescales. From the ternary diagram, we also observe that wave-dominated deltas appear to have lower rates of migration than fluvial-dominated deltas. There are several potential reasons for these trends we see to be occurring. It is possible that the daily cycle of inflowing tidal forces returning sediment that has flowed out of the channel is acting as a stabilizing force, inhibiting channel movement in tidal- vs. fluvial-dominated deltas (28). The observed larger migration rates in tidal- vs. wave-dominated deltas could be due to the fact that as tides propagate farther landward, distortion and asymmetry of tidal currents can develop and instigate morphological change more than waves that are on the coast (48, 49).

Without a larger dataset of deltas paired with process-based models of each deltas formation, we cannot conclusively state how the balance of waves, tides, and fluvial forces impacts the distribution of channel migration rates. However, we can make initial observations about the patterns that were observed in the set of 48 deltas that were included in this study. From the data in this study, we hypothesize that if all other aspects of a system were equivalent, the dominant forcing acting on a delta could be expected to determine the delta's capacity to effectively turn available water and sediment into channel movement. To some extent, river-dominated deltas would have a high capacity to create channel movement, tidal-dominated deltas would have a lower capacity to create channel movement, and wave-dominated deltas would have the lowest capacity for channel.

Sediment Flux and Flood Frequency. The presence of deltas with very low migration rates within the river-dominated portion of the triangle highlights the importance of considering other factors such as the magnitude of fluvial sediment flux (rather than the relative sediment flux) and flood frequency in conjunction with dominant processes. If a delta is river dominated and has a large potential capacity to create channel movement, it does not mean that channel movement is necessarily occurring. As discussed in the introduction, without adequate magnitude of sediment supply, morphological change cannot occur, regardless of the level of relative river forcing present in the system (50). This concept can be exemplified by examining the Dnieper delta, a delta with a strong relative river forcing of 98% that exhibits very low migration rates (0.66 m/y). Although the Dnieper delta has high potential to create channel movement with its strong relative river influence and absence of strong tidal and wave influence, it does not have the necessary water and sediment

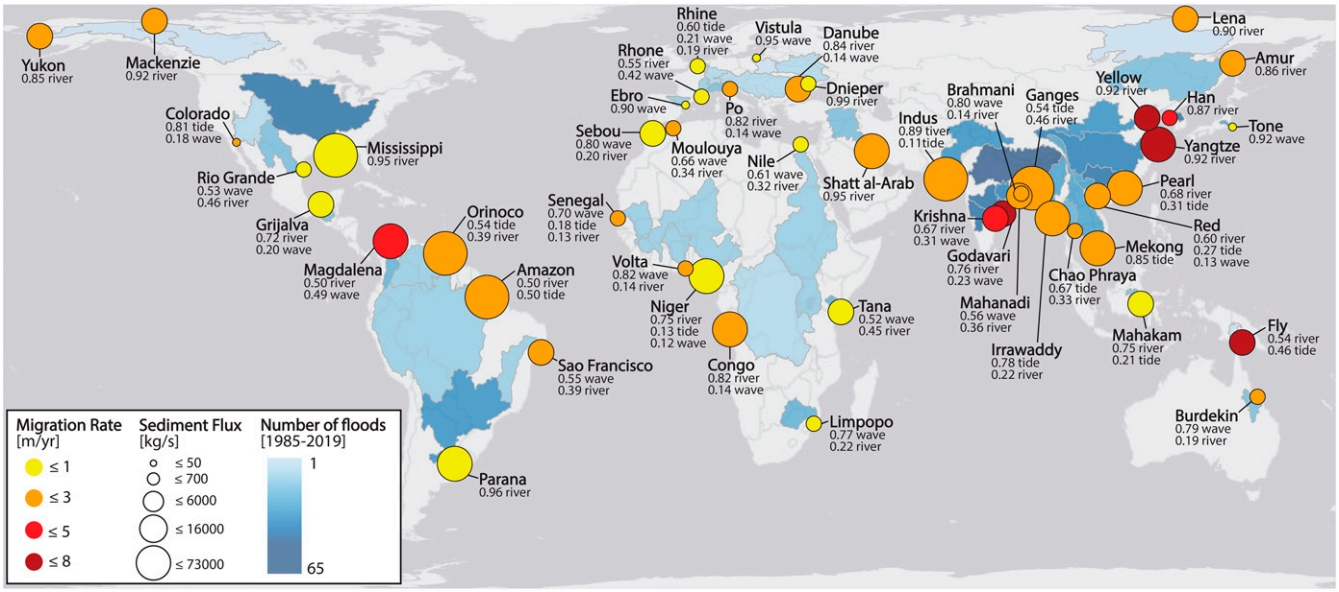

Fig. 2. Locations of each of the 48 deltas with information on median migration rate; magnitude of fluvial sediment flux; number of flood events occurring in the delta boundary from 1985 to 2019; and the balance of river, tidal, and wave forcings on each system. In deltas where there is a strong single dominant forcing greater than 0.85, only that forcing is displayed. The number of floods is represented by coloring the full watershed for visualization purposes. Full breakdown of the balance of forces and median migration rates can be found in *SI Appendix*, Table S1.

supply to create channel movement because of damming near the mouth of the river (51).

Combined Effects of All Variables. To examine how all three key forcings simultaneously interact and correlate to channel movement, a global map with each delta's geographic location, median migration rate, dominant processes of formation (22), magnitude of fluvial sediment flux (22), and flood frequency (52) is created (Fig. 2). In addition to the global map, a series of scatterplots has also been created to observe the basic correlation between each variable and the magnitude of median migration rate (*SI Appendix*, Fig. S1). These two visualizations reveal that delta systems with a combination of high flood frequency, high sediment flux, and high degrees of river forcing tend to have the highest rates of channel migration (e.g., Yellow, Yangtze, Godavari). This is in accordance with what we know about the individual effect of each of these parameters. Conversely, deltas with low flood frequency, low sediment flux, and low river forcing percentage tend to have the lowest amount of channel migration (e.g., Vistula, Ebro, Rhine, Tone). Systems with a mix of migration-enhancing features and migration-dampening features tend to fall into the intermediate migration rate bins. For example, the Ganges delta has large levels of sediment flux and is in a high–flood frequency zone, but its median migration rate is lowered by the fact that the Ganges has around 50% tidal forcing acting to stabilize channels. We observe that deltas with similar values of forcing, sediment flux, and flood frequency will often have similar migration rates. For instance, the Mackenzie and the Yukon deltas both have strong river forcing, have fluvial sediment flux magnitudes in the middle bin of values, have similar frequencies of flood events, and additionally, are in arctic climates. Correspondingly, the Mackenzie and the Yukon have nearly identical median migration rates of 1.04 and 1.08 m/y, respectively. However, there are some instances where deltas have similar values for dominant forcings, sediment flux, and flood frequency, yet they display differences in migration patterns. For these deltas, we must consider other factors that can have an impact on channel mobility.

Other Factors That Contribute to Channel Migration Values. One major factor to consider that can alter migration rates is the level of urbanization of a river delta. Deltas in highly urbanized environments are often engineered to manually control the movement of channels in order to protect the adjacent infrastructure. Structures such as embankments, levees, and retaining walls can all cause deviations from the migration rates we might expect due to the previously discussed forcings (dominant process, sediment flux, and flood frequency). One example of this is the Mississippi delta. The Mississippi has a strong river forcing, high flood frequency, and a relatively high sediment flux, yet it displays a very low median migration rate of just 0.89 m/y. This combination of forcing, flooding, and sediment flux should yield larger levels of channel migration if the patterns discussed above hold true. However, the Mississippi has an extensive system of man-made levees that constrain potential channel movement to a lower level than expected (53).

Local biome classification can also have an impact on channel migration rates. An arctic delta, for instance, could be expected to have decreased rates of channel migration when compared with a tropical delta with otherwise similar properties because of the stabilizing effect of permafrost in arctic environments (54, 55). We find that although the three arctic systems we examine in this study (Lena, Yukon, and Mackenzie) all have high rates of river forcing, they also fall into the lower bins of channel movement with median migration rates of 2.38, 1.08, and 1.04 m/y, respectively (Fig. 2 and *SI Appendix*, Table S1). While these lower rates of migration could be due to the lower frequency of recorded flood events, their arctic positioning could also impact channel mobility by adding stability to their channel banks.

The local composition of stratigraphy will have an impact on channel movement as well. Bedrock channels will be less erodible than alluvial channels, especially over the decadal timescales we use in this study (56). At shallow depths, the presence of vegetation along channel banks can act to stabilize channels and impede movement (31, 47, 57). Regions of uplifted terraces due to tectonic activity can also limit potential migration by creating a natural physical barrier (58). Variations in suspended sediment composition will have an effect on channel kinematics as well. It has been demonstrated using numerical and physical models that changing the composition and cohesion of incoming sediment will cause changes to delta morphology (59–63).

Discussion

Local Migration vs. System-Averaged Migration. While using the median migration rates for each system is a convenient way to compare overall differences in channel migration among deltas, it is important to note that the system-averaged migration will often differ from local migration measurements. This can be seen by plotting the entire box plot distribution of each delta's thousands of migration vectors (Fig. 3*A*), where, the interquartile range (IQR) represents the level of deviation from the median value. As an alternative method to visualize the differences in the channel migration distributions, the cumulative frequency distribution of each delta is also mapped (*SI Appendix*, Fig. S2). We find that as the median migration rate of the distribution increases, the IQR also increases, suggesting that high channel migration is always accompanied by areas of low channel migration.

Many of the systems we extracted are composed of thousands of individual channel reaches that can potentially be dozens of kilometers away from one another. If one of these systems has a small IQR, it is likely that all of the channels are displaying migration rates close to the characteristic median migration rate. However, if a system has a large IQR and many outlier values, the total area can be subdivided into separate sections, and the migration rate distribution of the section of interest can be examined. For instance, the Ganges delta is more than 80,000 km^2 in area and can be subdivided into four distinct zones that each have their own different set of forcings (17, 64). The braided zone, the fluvial zone, the Polders (an embanked tidal zone), and the Sundarbans (a protected mangrove forest in the tidal zone) have been shown to have measurably different levels of channel dynamics (15, 17). When a PIV analysis is conducted on each region individually, very different distributions of channel migration are obtained (Fig. 3*B*), exemplifying the need to account for the spatial variability of migration patterns in larger systems.

In addition to averaging spatially over the delta extent, we are also averaging the total migration temporally over each time period to create a comparable single value for each system. While migration rates are expressed in meters per year, the migration of channels in each system may not always be occurring in equal intervals over the entire time span. For instance, the Yellow River delta has a large median migration rate of 7.28 m/y that was obtained from comparing channel centerlines in 1986 and 2019. One reason that the Yellow delta migration rates are so high is because of a large avulsion that occurred between 1995 and 1997 on the distal region of the delta. So, while the time-averaged rate of migration over the 36 y of observation for the Yellow River delta is 7.28 m/y, actual individual yearly migration rates may be much larger or much smaller depending on which year of the time span is being investigated. To gain more information about the temporal distribution of channel movement, additional analysis of the full time series of channel migration can be conducted. The channelized response variance (CRV) metric has been shown to effectively capture channel kinematics from a time series of images (17, 65). By observing the CRV patterns of a delta system, the temporal distribution of the observed channel migrations can be determined (*SI Appendix*, Figs. S3–S5).

Finally, it is important to note that just because a delta is or is not experiencing channel migration over the 20 to 35 y of imagery we have available, it does not mean that that delta will necessarily maintain that level of channel migration over longer timescales. Some systems have timescales of geomorphic change that are much larger than the timescales we analyze in this study, effectively causing our analysis to omit those channel movements.

Normalizing Channel Migration by Channel Width. Another aspect of channel migration that is not globally addressed in this study is the fact that larger channels will have larger magnitudes of migration than smaller channels when the percentage of channel width change is the same. For example, 10 m of channel migration for a 30-m-wide channel could be considered a much more significant change than 10 m of channel migration for a 4-km-wide channel. When the migration rate of each delta is compared with its average channel width, we can see that there is some correlation between the size of a delta's channels and its median migration rate (*SI Appendix*, Fig. S6). One appropriate way to address this consideration is to normalize migration rates by channel size (19).

To determine the potential impact of channel width on channel migration, the migration rates of each of the physiographic zones of the Ganges delta were paired with channel width data from a previous study (64). By comparing the box plot distributions of the Ganges physiographic zones not normalized by channel width (Fig. 3*B*) and the box plot distributions of those same zones divided by the average channel width of each zone (*SI Appendix*, Fig. S7), one can see that normalizing by channel width can provide a new perspective on channel migration. For instance, before normalizing by channel width, the Poldered zone of the Ganges appears to have much smaller migration rates than the Fluvial zone of the Ganges. However, after the migration rates have been normalized by a mean channel width value for the zone, the distributions of migration rates for the Poldered (tidal) and Fluvial zones appear to be much more similar [agreeing with the results of Finotello et al. (19)]. This result demonstrates how width normalization can potentially change research conclusions. On the other hand, this analysis also revealed that when normalized by channel width, the tidal Sundarbans zone (an area protected from human development) still had lower overall migration rates than the tidal Poldered zone (and any other zone of the Ganges), reinforcing the same results of the nonnormalized migration rate analysis.

This Ganges delta analysis exhibits that when adequate data on channel width are available, channel width normalization can reveal important aspects of delta channel kinematics. While sufficient channel width information to analyze migration normalized by channel width was available for the Ganges delta, the currently available global dataset of channel river widths that was used to create *SI Appendix*, Fig. S6 (66) does not encompass the same set of channels extracted for the PIV migration analysis. Additionally, while it is valid to consider channel migrations normalized by width of the channel to focus on the relative geomorphic impact, the focus of this study is to quantify how overall levels of migration may impact those living on delta systems, regardless of the relative channel sizes. For these reasons, we have chosen to report global migration rates in their full magnitude, not normalized by channel width. With the development of a global dataset of channel widths that encompasses the full coastal extent of channels, it will become possible to compare width-normalized channel migration globally and identify potentially anomalously mobile systems.

Using Existing Patterns to Inform Future Changes in Migration. Several datasets exist that analyze how flood frequency, sediment flux, and the balance of river, tidal, and wave forcings may change over time in river deltas. By combining these future scenarios with what we know about drivers of channel mobility, we can make better-educated guesses about how channel migration patterns will potentially change in each delta system in the future. This information could be vital to communities living on coastal delta systems as management decisions are made on local and national scales. The observations we have made in this report can serve as a starting point for further improving upon our predictive capacity of river delta kinematics.

In Hirabayashi et al. (67), global projected changes to flood frequency over the next century are calculated. Flood frequency is expected to increase in most parts of Europe and North America, as well as in the southernmost part of South America.

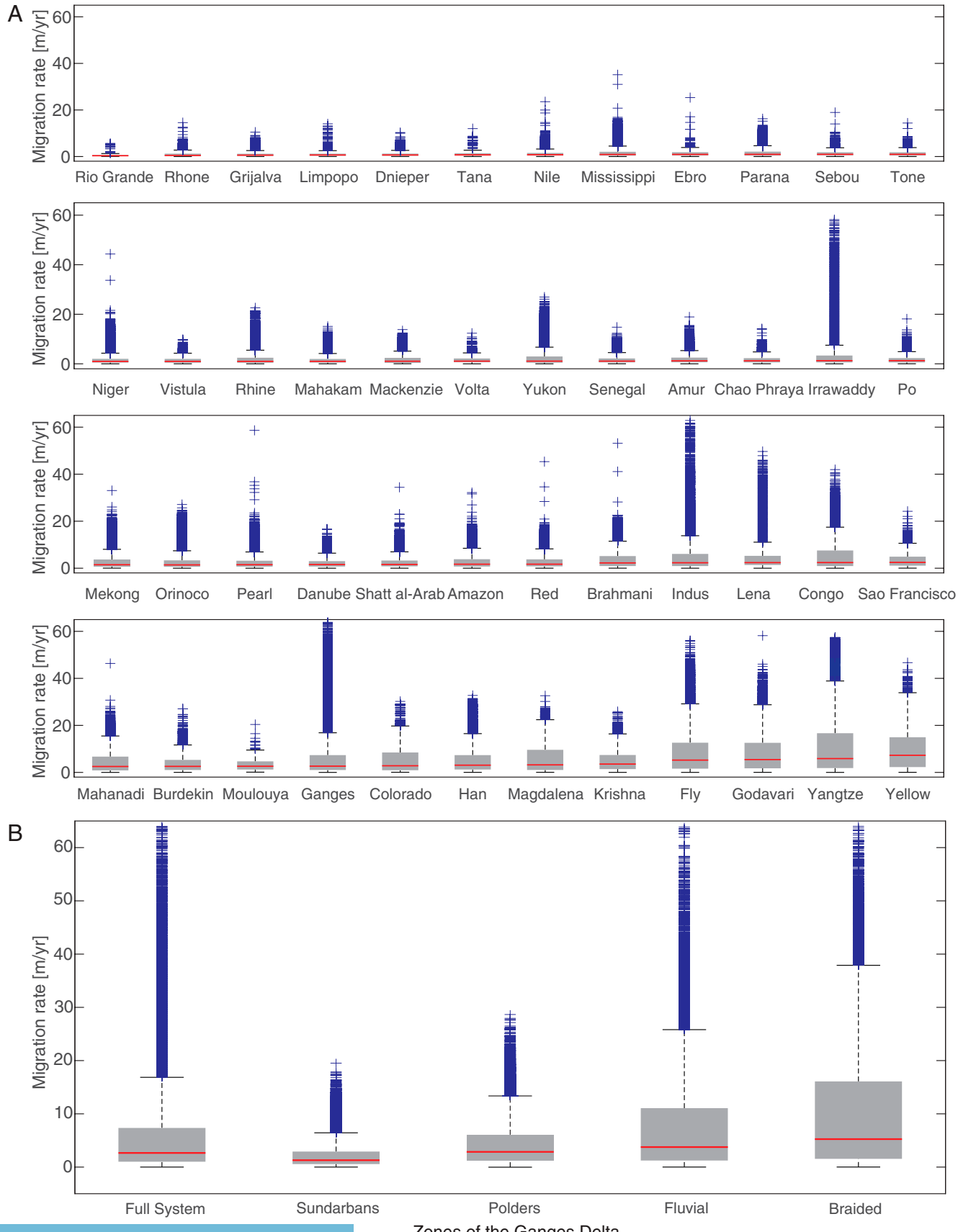

Fig. 3. Box plot distributions of (*A*) all 48 systems examined in this study and (*B*) each of the physiographic zones of the Ganges delta.

If the observations from this study are to hold in the future, these potential increases in flood frequency could result in corresponding increases in channel mobility in systems such as the Yukon, Mississippi, Ebro, Rhone, Po, Vistula, Dnieper, and Danube.

Future changes to global deltaic sediment flux under various climate change scenarios have been modeled by Dunn et al. (25). By comparing the current sediment flux values of each delta with the modeled sediment flux values for 100 y from now, we can inform predictions for which delta systems may have increases or decreases in their channel migration. After adjusting the sediment flux values for each of the 48 systems of this study by the percentages modeled in the study (25), we find that the Mississippi, Orinoco, and Lena may experience increases in sediment flux large enough to change their classification based on the bins we have defined in this study (*SI Appendix*, Fig. S8). These increases in sediment flux could potentially result in increases to the channel migration rates for these three systems. Similarly, we find that the Parana, Niger, Congo, Godavari, Mahanadi, Brahmani, Irrawaddy, Mekong, and Yangtze deltas are modeled as decreasing their sediment flux values, which could result in decreased rates of channel migration.

Finally, modeled changes to the balance of river, tidal, and wave forcings could be used to predict future trends in the location of deltas on Galloway's triangle (21). In Nienhuis et al. (22), a set of more than 10,000 deltas was analyzed to determine how each system's sediment flux values have changed under pristine and disturbed conditions. By identifying each of our 48 systems in this larger dataset and identifying which systems are becoming more or less river dominated, we can make predictions about changes to channel migration rates in each system. For instance, the Yellow River delta was modeled and determined to have a relative river forcing of nearly 100% under pristine conditions and closer to 92% under disturbed conditions (22). If this trend was to continue into the future, we might expect the Yellow River delta to become less and less river dominated, which could in turn cause a decrease in the rates of channel migration.

As our global classification has shown, the levels of river forcing, sediment flux, and flood frequency alone are not sufficient to definitively determine how mobile a network of channels will be. There are several other factors that we have discussed that can impact the mobility of channels across multiple scales. However, knowledge about the current and future values of these parameters combined with the findings of this study can provide a starting point for predicting how deltas will change and evolve in the future.

Conclusions

Hundreds of millions of people inhabit river deltas because of their fertile soil, ecologic diversity, and proximity to coastal navigational pathways. For these people, it is critically important to characterize the current morphological changes that have been occurring on delta networks over the last three decades. In this study, we have demonstrated that although some river deltas are static, a large portion of deltas are experiencing observable channel movements. By leveraging deep learning and principles of PIV, a methodology for the automatic extraction of channel migration vectors from remotely sensed imagery was created and implemented to obtain an accurate and spatially dense representation of channel migration in each of the 48 river deltas in our study. We have created a global dataset characterizing the spatial distribution of delta channel migration over decadal timescales. By observing correlation between our migration dataset and various common forcings on delta systems, we were able to observe the global role tides and waves play in stabilizing delta channels as compared with fluvial forces and observe that increases in sediment flux and flood frequency correlate to increased rates of channel migration. In the future, these initial observations could be expanded and paired with a sensitivity analysis using process-based morphodynamic models to develop a fully predictive model for deltaic channel migration.

The results produced in this study can be used for informing and validating numerical models, interpreting fluvial stratigraphy, aiding in engineering operations decision making, and predicting future changes to delta channel dynamics in response to changing forcings. Finally and arguably most importantly, if the spatial distribution of channel migration rates determined in this study was to be disseminated on the local scale to those actually living on these systems, it could provide invaluable information to help locals make everyday decisions.

While some morphological changes occur over millennial timescales, the channel migration rates that we observe and quantify in this study are occurring over decadal timescales that are highly relevant to those inhabiting these systems. A greater understanding of delta channel migration rates as they compare with one another globally, as well as how they vary within large systems, is very important to have as we continue to work toward deltaic sustainability. With proper planning and information like that provided in this study, we can work toward creating a balance between human habitation and the natural dynamic behavior of river delta channels.

Materials and Methods

Extracting Delta Centerlines from Imagery. The set of 48 deltas is chosen in alignment with previous global datasets of delta systems (23–25). Multispectral images for the first and last clean images of each delta system are obtained using Google Earth Engine Code Editor (68). Geographic extents for each system are obtained by using the extents previously defined in the supplementary information of Tessler et al. (23). Final multispectral images are created by compositing all cloud-free images from the 6 driest months of the year for each particular system (Fig. 4*A*). Including 6 mo of imagery rather than simply using a single image has been shown to dampen unavoidable potential fluctuations in tidal levels (17).

Multispectral imagery is converted to water probability maps by using DeepWaterMap, a fully convolutional neural network that has been trained to distinguish water presence from land, ice, snow, clouds, and shadows (40). The newest release of DeepWaterMap has been modified to allow the tool to "see through" small clouds, increasing the accuracy of the extracted water maps (41). The water probability map is then converted to a binary water map using Otsu thresholding (70) (Fig. 4*B*). Centerlines are extracted from the binary water maps using the MATLAB function "bwskel," a morphological operator that extracts channel centerlines while preserving the object Euler number (42) (Fig. 4*B*).

PIV Analysis. After a centerline network has been obtained for both the first and the last years of imagery available in each delta, centerline networks are loaded into PIVLab, a MATLAB-based software that uses principles of PIV in order to determine the most probabilistic displacement for objects and create velocity vectors to represent that displacement (69). Velocity vectors are created by evaluating the cross-correlation of smaller subsections of the image (interrogation areas), where the point of highest correlation corresponds to the most probable displacement of the interrogation area between time 1 and time 2 (Fig. 4 *C* and *E*). Vectors are then converted to a raster Geostationary Earth Orbit Tagged Image File Format (GeoTIFF) format so that migration rates can be loaded into maps for analysis (Fig. 4*D*). We find that this PIV tool is capable of capturing various forms of channel movement at different scales and at a dense spatial resolution (Fig. 4*E*). We are able to confirm the effectiveness of PIV in tracking channel centerline movement by comparing PIV-derived migration trends with previously studied kinematics of the Ganges delta. In a previous study of the Ganges delta, we analyzed the variance of a time series of channel maps and found that the Sundarbans, a tidal mangrove forest protected from anthropogenic interference, had low magnitudes of channel variance (17). By subdividing the Ganges into its separate physiographic zones and repeating the same analysis, it was revealed that the Sundarbans zone had the least channel variance, the embanked tidal zone (Polders) had the second least channel variance, the fluvial forced zone had the third least channel variance, and the braided section of the delta had the highest magnitudes of channel variance (17). When we conducted a PIV analysis of each of the Ganges zones, we were

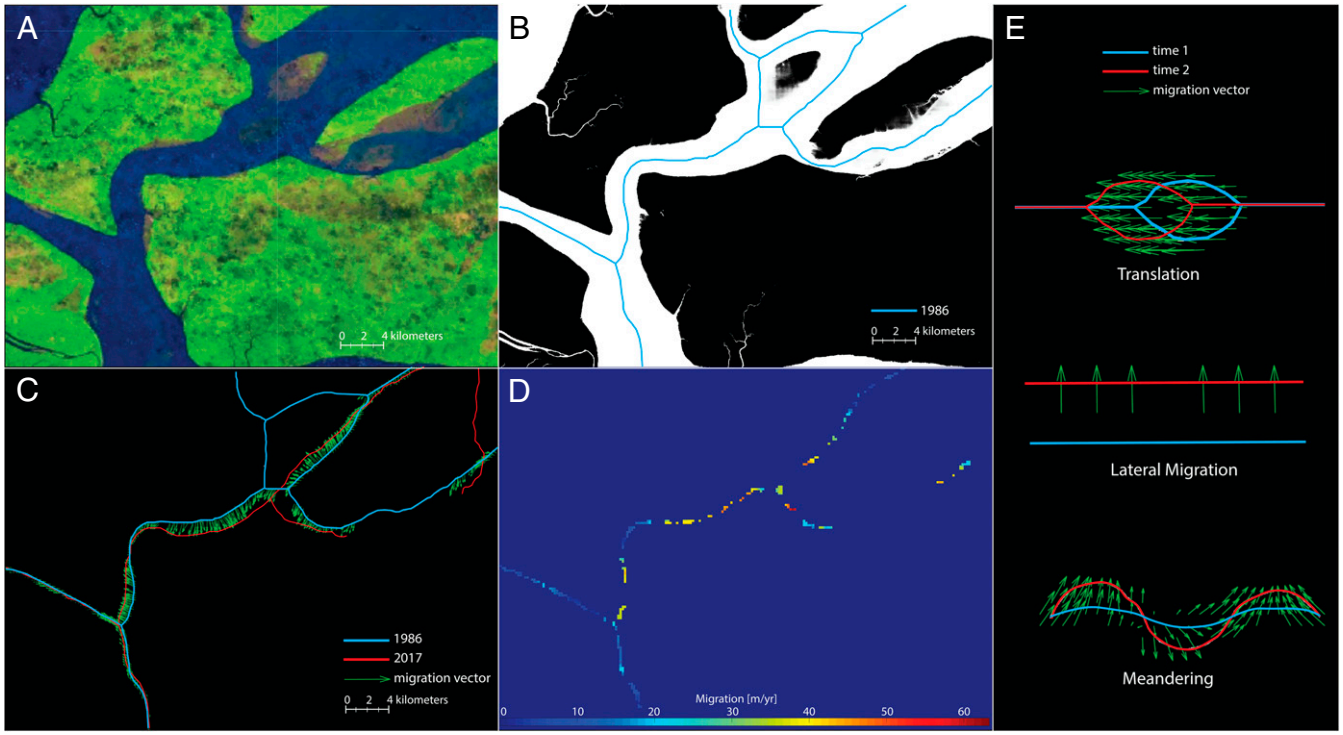

Fig. 4. Methodology demonstrated using a small subsection of the Amazon as an example. (*A*) The multispectral image is converted to a (*B*) binary water map with centerlines extracted using a morphological operator. (*C*) PIVLab-generated migration vectors for the subsection of the Amazon River delta evolution between 1986 (blue) and 2017 (red). (*D*) The migration magnitudes derived from the migration vectors. (*E*) An example of three migration mechanisms of synthetically derived centerlines that are captured using PIVLab (69).

able to extract the same trends in channel dynamics (Fig. 3*B*), demonstrating that PIV is able to capture expected differences in channel migration.

The four interrogation area parameters for the PIV analysis were chosen as 128, 64, 32, and 16 pixels. A large initial interrogation area is chosen to allow the technique to capture large migration magnitudes. The initial 128-pixel interrogation area is given a step size of 64 pixels, meaning that the maximum potential migration that is capable of being extracted in this analysis is 64 pixels per frame (1,920 m per "x" years). The minimum interrogation area was chosen as 16 pixels in order to ensure that there were enough occupied pixels in each frame to successfully calculate the cross-correlation. Different interrogation area specifications may yield slightly different migration rate distributions; however, because we used the same parameters for each of the 48 delta systems, the extracted migration rates are highly comparable. The correlation between interrogation areas is calculated using the discrete Fourier transform option in PIVLab in order to increase the signal to noise ratio and to account for nonuniform motion of the centerlines within the interrogation area (71). Large channel movements that surpass this maximum migration rate of 64 pixels per frame, such as avulsions, will not be fully captured by this technique. Additionally, if no clear peak in the correlation matrix can be found between interrogation areas, no migration vector is created. These two aspects of the PIV analysis result in conservative estimations for channel migration. More information on the underlying PIVLab methodology used in this analysis is in the works by Thielicke and Stamhuis (69) and Thielicke (71). Raster files representing each of the 48 deltas centerline migration rates are available at https://osf.io/x7k53/. To demonstrate the format of these raster files, four examples of the migration rate spatial distributions are included in *SI Appendix* (*SI Appendix*, Fig. S9).

Obtaining Global Forcing Data. To obtain values for the relative wave, fluvial, and tidal influence, the sediment flux data from Nienhuis et al. (22) were obtained for each of the 48 deltas in this study. To obtain information on the magnitude of sediment flux for each system, the disturbed fluvial sediment flux values for each system were also obtained from Nienhuis et al. (22). Flood frequency values for each delta were obtained by leveraging data from the Dartmouth Flood Observatory Archive (52). In this dataset, shape files representing each documented major flood event from 1985 to the present are available. To count the number of major floods in each delta, the shape files of flood event extents and delta area were overlapped, and the number of floods intercepting each delta area was counted.

Data Availability. GeoTIFFs data have been deposited in the Open Science Framework (https://osf.io/x7k53/) (72). Methods are freely available at MathWorks, https://www.mathworks.com/matlabcentral/fileexchange/27659-pivlab-particle-image-velocimetry-piv-tool-with-gui and GitHub, https://github.com/passaH2O/CRV-Analysis. Imagery used in this paper is freely available online using the Google Earth Engine Code Editor (68).

ACKNOWLEDGMENTS. This material is based on work supported by NSF Grants OCE-1600222 (to P.P.), CAREER-1350336 (to P.P.), and EAR-1642611 (to P.P.) and by Planet Texas 2050, a research grant challenge at the University of Texas at Austin. Comments received from the Editor and three anonymous reviewers helped improve this manuscript.

1. R. Slingerland, N. D. Smith, River avulsions and their deposits. *Annu. Rev. Earth Planet. Sci.* **32**, 257–285 (2004).
2. D. J. Jerolmack, D. Mohrig, Conditions for branching in depositional rivers. *Geology (Boulder)* **35**, 463–466 (2007).
3. J. Martin, B. Sheets, C. Paola, D. Hoyal, Influence of steady base-level rise on channel mobility, shoreline migration, and scaling properties of a cohesive experimental delta. *J. Geophys. Res.* **114**, F03017 (2009).
4. A. Hoitink, Z. Wang, B. Vermeulen, Y. Huismans, K. Kästner, Tidal controls on river delta morphology. *Nat. Geosci.* **10**, 637–645 (2017).
5. L. Giosan, J. Syvitski, S. Constantinescu, J. Day, Climate change: Protect the world's deltas. *Nature* **516**, 31–33 (2014).
6. D. A. Edmonds, R. L. Caldwell, E. S. Brondizio, S. M. O. Siani, Coastal flooding will disproportionately impact people on river deltas. *Nat. Commun.* **11**, 4741 (2020).
7. V. K. Gupta, O. J. Mesa, Runoff generation and hydrologic response via channel network geomorphology: Recent progress and open problems. *J. Hydrol. (Amst.)* **102**, 3–28 (1988).
8. L. Benda *et al.*, The network dynamics hypothesis: How channel networks structure riverine habitats. *Bioscience* **54**, 413–427 (2004).
9. L. Benda, K. Andras, D. Miller, P. Bigelow, Confluence effects in rivers: Interactions of basin scale, network geometry, and disturbance regimes. *Water Resour. Res.* **40**, W05402 (2004).

10. B. Biswal, M. Marani, Geomorphological origin of recession curves. *Geophys. Res. Lett.* **37**, L24403 (2010).
11. I. Zaliapin, E. Foufoula-Georgiou, M. Ghil, Transport on river networks: A dynamic tree approach. *J. Geophys. Res. Earth Surf.* **115**, F00A15 (2010).
12. J. A. Czuba, E. Foufoula-Georgiou, A network-based framework for identifying potential synchronizations and amplifications of sediment delivery in river basins. *Water Resour. Res.* **50**, 3826–3851 (2014).
13. P. F. Hudson, R. H. Kesel, Channel migration and meander-bend curvature in the lower Mississippi river prior to major human modification. *Geology (Boulder)* **28**, 531–534 (2000).
14. J. A. Constantine, T. Dunne, J. Ahmed, C. Legleiter, E. D. Lazarus, Sediment supply as a driver of river meandering and floodplain evolution in the amazon basin. *Nat. Geosci.* **7**, 899–903 (2014).
15. C. Wilson *et al.*, Widespread infilling of tidal channels and navigable waterways in the human-modified tidal delta plain of southwest Bangladesh. *Elementa Sci. Anthropocene* **5**, 78 (2017).
16. Z. Sylvester, P. Durkin, J. A. Covault, High curvatures drive river meandering. *Geology* **47**, 263–266 (2019).
17. T. Jarriel, L. F. Isikdogan, A. Bovik, P. Passalacqua, System wide channel network analysis reveals hotspots of morphological change in anthropogenically modified regions of the Ganges Delta. *Sci. Rep.* **10**, 12823 (2020).
18. P. Passalacqua, L. Giosan, S. Goodbred, I. Overeem, Stable ≠ sustainable: Delta network dynamics versus the human need for stability. *Earths Futue* **9**, e2021EF00212 (2021).
19. A. Finotello *et al.*, Field migration rates of tidal meanders recapitulate fluvial morphodynamics. *Proc. Natl. Acad. Sci. U.S.A.* **115**, 1463–1468 (2018).
20. M. Donovan, P. Belmont, Timescale dependence in river channel migration measurements. *Earth Surf. Process. Landf.* **44**, 1530–1541 (2019).
21. W. Galloway, "Process framework for describing the morphologic and stratigraphic evolution of deltaic depositional system" in *Deltas, Models for Exploration*, M. L. Broussard, Ed. (Houston Geological Society, 1975), pp. 86–98.
22. J. H. Nienhuis *et al.*, Global-scale human impact on delta morphology has led to net land area gain. *Nature* **577**, 514–518 (2020).
23. Z. D. Tessler *et al.*, ENVIRONMENTAL SCIENCE. Profiling risk and sustainability in coastal deltas of the world. *Science* **349**, 638–643 (2015).
24. Z. D. Tessler, C. J. Vörösmarty, I. Overeem, J. P. Syvitski, A model of water and sediment balance as determinants of relative sea level rise in contemporary and future deltas. *Geomorphology* **305**, 209–220 (2018).
25. F. E. Dunn *et al.*, Projections of declining fluvial sediment delivery to major deltas worldwide in response to climate change and anthropogenic stress. *Environ. Res. Lett.* **14**, 084034 (2019).
26. S. Fagherazzi, Self-organization of tidal deltas. *Proc. Natl. Acad. Sci. U.S.A.* **105**, 18692–18695 (2008).
27. V. M. Rossi *et al.*, Impact of tidal currents on delta-channel deepening, stratigraphic architecture, and sediment bypass beyond the shoreline. *Geology* **44**, 927–930 (2016).
28. N. Lentsch, A. Finotello, C. Paola, Reduction of deltaic channel mobility by tidal action under rising relative sea level. *Geology* **46**, 599–602 (2018).
29. G. Nanson, E. J. Hickin, Channel migration and incision on the Beatton river. *J. Hydraul. Eng.* **109**, 327–337 (1983).
30. T. Dunne, J. A. Constantine, M. Singer, The role of sediment transport and sediment supply in the evolution of river channel and floodplain complexity. *Transactions. Japanese Geomorphol. Union* **31**, 155–170 (2010).
31. A. D. Wickert *et al.*, River channel lateral mobility: Metrics, time scales, and controls. *J. Geophys. Res. Earth Surf.* **118**, 396–412 (2013).
32. J. Hooke, An analysis of the processes of river bank erosion. *J. Hydrol. (Amst.)* **42**, 39–62 (1979).
33. J. M. Hooke, Magnitude and distribution of rates of river bank erosion. *Earth Surf. Processes* **5**, 143–157 (1980).
34. R. H. Kesel, R. H. Baumann, Bluff erosion of a Mississippi river meander at Port Hudson, Louisiana. *Phys. Geogr.* **2**, 62–82 (1981).
35. M. Gharbi, A. Soualmia, D. Dartus, L. Masbernat, Floods effects on rivers morphological changes application to the Medjerda river in Tunisia. *J. Hydrol. Hydromech.* **64**, 56–66 (2016).
36. J. Lewin, Initiation of bed forms and meanders in coarse-grained sediment. *Geol. Soc. Am. Bull.* **87**, 281–285 (1976).
37. S. Ikeda, G. Parker, K. Sawai, Bend theory of river meanders. Part 1. Linear development. *J. Fluid Mech.* **112**, 363–377 (1981).
38. W. E. Dietrich, J. D. Smith, T. Dunne, Flow and sediment transport in a sand bedded meander. *J. Geol.* **87**, 305–315 (1979).
39. C. A. Braudrick, W. E. Dietrich, G. T. Leverich, L. S. Sklar, Experimental evidence for the conditions necessary to sustain meandering in coarse-bedded rivers. *Proc. Natl. Acad. Sci. U.S.A.* **106**, 16936–16941 (2009).
40. F. Isikdogan, A. C. Bovik, P. Passalacqua, Surface water mapping by deep learning. *IEEE J. Sel. Top. Appl. Earth Obs. Remote Sens.* **10**, 4909–4918 (2017).
41. L. F. Isikdogan, A. Bovik, P. Passalacqua, Seeing through the clouds with deepwater map. *IEEE Geosci. Remote Sens. Lett.* **17**, 1662–1666 (2020).
42. MATLAB, *9.7.0.1190202 (R2019b)* (The MathWorks Inc., Natick, MA, 2018).
43. J. Westerweel, G. E. Elsinga, R. J. Adrian, Particle image velocimetry for complex and turbulent flows. *Annu. Rev. Fluid Mech.* **45**, 409–436 (2013).
44. E. Hickin, The development of meanders in natural river-channels. *Am. J. Sci.* **274**, 414–442 (1975).
45. J. M. Hooke, C. Redmond, *Use of Cartographic Sources for Analysing River Channel Change with Examples from Britain* (Wiley, Chichester, United Kingdom, 1989).
46. E. J. Hickin, G. C. Nanson, Lateral migration rates of river bends. *J. Hydraul. Eng.* **110**, 1557–1567 (1984).
47. E. R. Micheli, J. W. Kirchner, E. W. Larsen, Quantifying the effect of riparian forest versus agricultural vegetation on river meander migration rates, Central Sacramento River, California, USA. *River Res. Appl.* **20**, 537–548 (2004).
48. S. Lanzoni, G. Seminara, Long-term evolution and morphodynamic equilibrium of tidal channels. *J. Geophys. Res. Ocean* **107**, 1-1-1-13 (2002).
49. M. Bolla Pittaluga *et al.*, Where river and tide meet: The morphodynamic equilibrium of alluvial estuaries. *J. Geophys. Res. Earth Surf.* **120**, 75–94 (2015).
50. J. M. Swartz, T. A. Goudge, D. C. Mohrig, Quantifying coastal fluvial morphodynamics over the last 100 years on the lower Rio Grande, USA and Mexico. *J. Geophys. Res. Earth Surf.* **125**, 5e2019JF005443 (2020).
51. V. Timchenko, O. Oksiyuk, J. Gore, A model for ecosystem state and water quality management in the Dnieper river delta. *Ecol. Eng.* **16**, 119–125 (2000).
52. G. R. Brackenridge, Global Active Archive of Large Flood Events, Dartmouth Flood Observatory, University of Colorado, USA. http://floodobservatory.colorado.edu/Archives. Accessed 1 June 2021.
53. F. Vahedifard, S. Sehat, J. V. Aanstoos, Effects of rainfall, geomorphological and geometrical variables on vulnerability of the lower Mississippi river levee system to slump slides. *Georisk* **11**, 257–271 (2017).
54. R. Lauzon, A. Piliouras, J. C. Rowland, Ice and permafrost effects on delta morphology and channel dynamics. *Geophys. Res. Lett.* **46**, 6574–6582 (2019).
55. A. Piliouras, J. C. Rowland, Arctic river delta morphologic variability and implications for riverine fluxes to the coast. *J. Geophys. Res. Earth Surf.* **125**, 6e2019JF005250 (2020).
56. J. M. Turowski, *Semi-Alluvial Channels and Sediment-Flux-Driven Bedrock Erosion in Gravel-Bed Rivers* (John Wiley and Sons, Ltd, Chichester, United Kingdom, 2012), pp. 399–418.
57. A. Ielpi, M. G. Lapôtre, A. Finotello, M. Ghinassi, A. D'Alpaos, Channel mobility drives a diverse stratigraphic architecture in the dryland Mojave River (California, USA). *Earth Surf. Process. Landf.* **45**, 1717–1731 (2020).
58. R. Kalliola *et al.*, Upper amazon channel migration: Implications for vegetation perturbance and succession using bitemporal Landsat MSS images. *Naturwissenschaften* **79**, 75–79 (1992).
59. D. A. Edmonds, R. L. Slingerland, Mechanics of river mouth bar formation: Implications for the morphodynamics of delta distributary networks. *J. Geophys. Res. Earth Surf.* **112**, F02034 (2007). Correction in: *J. Geophys. Res. Earth Surf.* **112**, F03099 (2007).
60. N. Geleynse *et al.*, Controls on river delta formation: Insights from numerical modelling. *Earth Planet. Sci. Lett.* **302**, 217–226 (2011).
61. R. L. Caldwell, D. A. Edmonds, The effects of sediment properties on deltaic processes and morphologies: A numerical modeling study. *J. Geophys. Res. Earth Surf.* **119**, 961–982 (2014).
62. A. Tejedor *et al.*, Quantifying the signature of sediment composition on the topologic and dynamic complexity of river delta channel networks and inferences toward delta classification. *Geophys. Res. Lett.* **43**, 3280–3287 (2016).
63. M. Liang, C. Van Dyk, P. Passalacqua, Quantifying the patterns and dynamics of river deltas under conditions of steady forcing and relative sea level rise. *J. Geophys. Res. Earth Surf.* **121**, 465–496 (2016).
64. P. Passalacqua, S. Lanzoni, C. Paola, A. Rinaldo, Geomorphic signatures of deltaic processes and vegetation: The Ganges-Brahmaputra-Jamuna case study. *J. Geophys. Res. Earth Surf.* **118**, 1838–1849 (2013).
65. T. Jarriel, L. F. Isikdogan, A. Bovik, P. Passalacqua, Characterization of deltaic channel morphodynamics from imagery time series using the channelized response variance. *J. Geophys. Res. Earth Surf.* **124**, 3022–3042 (2019).
66. G. H. Allen, T. M. Pavelsky, Global extent of rivers and streams. *Science* **361**, 585–588 (2018).
67. Y. Hirabayashi *et al.*, Global flood risk under climate change. *Nat. Clim. Chang.* **3**, 816–821 (2013).
68. N. Gorelick *et al.*, Google Earth Engine: Planetary-scale geospatial analysis for everyone. *Remote Sens. Environ.* **202**, 18–27 (2017).
69. W. Thielicke, E. J. Stamhuis, Pivlab–towards user-friendly, affordable and accurate digital particle image velocimetry in MATLAB. *J. Open Res. Softw.* **2**, e30–e30 (2014).
70. N. Otsu, A threshold selection method from gray-level histograms. *IEEE Trans. Syst. Man Cybern.* **9**, 62–66 (1979).
71. W. Thielicke, "The flapping flight of birds - analysis and application," PhD thesis, University of Groningen, Groningen, The Netherlands (2014).
72. T. Jarriel, J. Swartz, P. Passalacqua, Global rates and patterns of channel migration in river deltas - Supplementary Data. Open Science Framework. https://osf.io/x7k53/. Deposited 20 September 2021.